Effect of Hub Clearance on Performance of Radial Turbine

R. D. Bharathan, P. Manigandan, Sharad Kapil, S. V. Ramana Murty, and D. Kishore Prasad

Abstract Scalloping of turbine wheel blisk of a radial turbine is done to reduce the centrifugal stress on the disc portion of the blisk, reduce weight and to decrease turbo lag in turbochargers. An attempt has been made to model the effect of scalloping of the turbine wheel on the performance of the radial turbine. The scallops have been modelled as hub clearances and analyses with various depths of scalloping and hub clearances have been analyzed using commercial 3D NS solver. The decrease in efficiency with increased scalloping and hub clearances has been plotted, and the results have been qualitatively compared with experimental results of similar but different radial turbines with and without scalloping. The results of the analyses are found to follow the same trend as those of the experiments.

Keywords Scalloping · Partial hub clearance · Tip clearances · Rotor blisk and twin scroll volute

Nomenclature

C_p	Mean specific heat capacity, J/kg-K
C0	Spouting velocity, m/s
C3	Rotor outlet mean absolute speed, m/s
M	Mach number

R. D. Bharathan (✉) · P. Manigandan · S. Kapil · S. V. Ramana Murty · D. Kishore Prasad
DRDO—Gas Turbine Research Estabilishment, Bengaluru, India
e-mail: bharathan.gtre@gov.in

S. Kapil
e-mail: sharadkapil.gtre@gov.in

S. V. Ramana Murty
e-mail: ramanamurthy.gtre@gov.in

D. Kishore Prasad
e-mail: kishoreprasadd.gtre@gov.in

G. Sivaramakrishna et al. (eds.), *Proceedings of the National Aerospace Propulsion Conference*, Lecture Notes in Mechanical Engineering,
https://doi.org/10.1007/978-981-19-2378-4_7

N	Rotational speed, rpm
Ns	Specific speed, radian
PS	Pressure Side
R2	Rotor inlet radius, mm
R3h	Rotor outlet hub radius, mm
R3s	Rotor outlet tip radius, mm
R_C	Volute corner radius, mm
R_{MAIN}	Volute main radius, mm
R_s	Volute scroll wall radius, mm
S	Blade pitch, mm
SS	Suction side
T_{in}	Inlet total temperature, K
T_{max}	Maximum thickness
U2	Rotor inlet mean blade speed, m/s
V2	Rotor inlet mean relative speed, m/s
V3	Rotor outlet mean relative speed, m/s
W	Mass flow rate, kg/s
Wax	Axial rotor width, mm
b2	Rotor inlet width, mm
ts	Scroll wall thickness, mm
ΔT	Temperature drop across turbine, K
δ	Volute section half angle, deg

1 Introduction

The radial turbine of a turbocharger performs the function of extracting power from the exhaust gases of the internal combustion engine in order to power the centrifugal compressor through a shaft. For its part, the compressor compresses the air at the inlet to the engine and so enhances the engine's volumetric efficiency. A typical vane-less radial turbine comprises a volute and rotor. The exhaust gases from the engine are accelerated by the volute and fed to the rotor the required inlet Mach number and flow angle with the least possible variation of flow properties along the circumferential direction. The gases in turn expand in the rotor, and thus, power is extracted.

Euler's turbine equation states that power extracted by the turbine is as follows:

$$\text{Power} = W(U2 * C2_{\text{swirl}} - U3 * C3_{\text{swirl}}) \tag{1}$$

Power extraction in a radial turbine wheel happens both through reduction in blade speed through reduction in radius from inlet to outlet and through a reduction in swirl velocity. The part of the turbine wheel that has the highest radius is its inlet. Most turbocharger turbine wheels are produced as integral blisks through casting route.

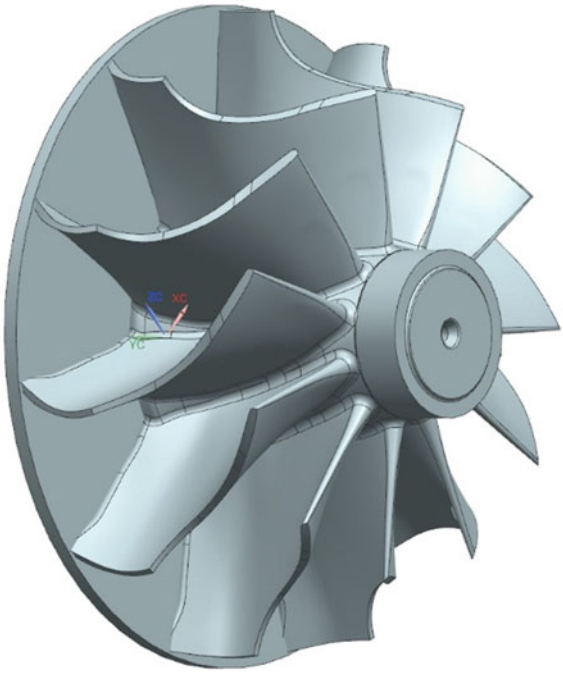

Fig. 1 Turbine wheel without scalloping

As the temperature of exhaust gases from the engine is high, they are made of nickel-based superalloys to withstand the high temperature and to meet the life requirement. Therefore, they are typically heavier than the centrifugal impeller and shaft. Excess weight in the inlet hub location which forms the hub endwall of the turbine wheel can lead to high centrifugal stresses on its solid disc portion; see Fig. 1. It can also increase the moment of inertia of the wheel which can lead to a slow response to accelerations and decelerations of the engine, also known as turbo lag; see [1].

In order to reduce the centrifugal stresses in the disc portion of the turbine wheel and to reduce turbo lag, the hub endwalls at the inlet between turbine blades are scooped out by introducing scallops between them as shown in Fig. 2. The stationary heat shield which protects the bearing housing and shaft from the hot turbine gases also performs the function of an endwall separated from the turbine wheel by an axial clearance which shall henceforth be called hub clearance as shown in Fig. 3.

The scalloping of the turbine wheel is accompanied by reduction in efficiency of the radial turbine because, similar to what happens in the tip clearance region, the introduction of a hub clearance provides a short cut for the gases to flow across the clearance from pressure side to suction side which leads to vortices which increase the losses in the stage which translated to a reduction in turbine efficiency. If maps of the radial turbine generated through analysis do not cater to the effect of scalloping, they may lead to overestimation of the performance of the turbine and erroneous matching of radial turbine with centrifugal compressor. Therefore, it is important to

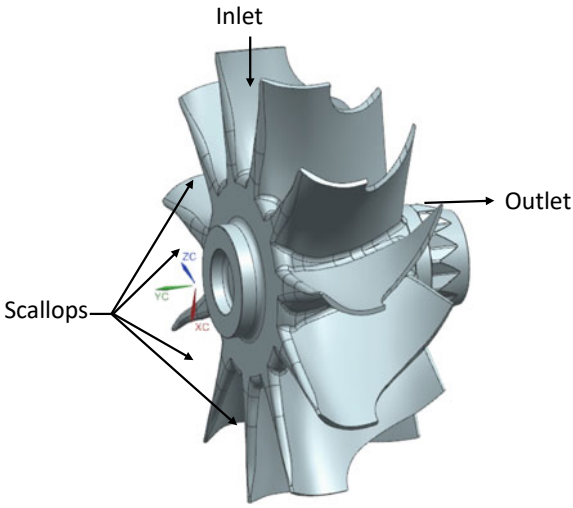

Fig. 2 Scalloped turbine wheel

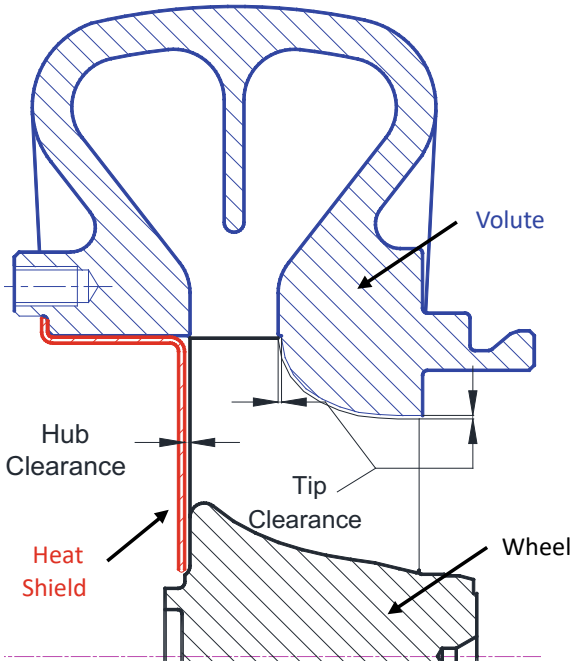

Fig. 3 Radial turbine stage

qualitatively and quantitatively understand the effect of scalloping and hub clearance on the aerodynamic performance of a radial turbine.

2 Description of Radial Turbine Stage

The design of the radial turbine under study was explained in [2]. The methodology for mean-line design of the radial turbine volute and wheel is provided in [3–5]. A vane-less design is favored because of the reduction in part count and weight as well as increase in reliability. To harness the effect of pulsation from the engine cylinders which fire in sequence, a twin scroll volute was designed as discussed in [1]. Appropriate cut-water angle was chosen based on producibility and aerodynamic consideration; see [6]. Table 1 gives the non-dimensional design parameters:

A previously designed and tested rotor wheel is analyzed using an analysis code developed based on [7]. Figure 4 shows the flow path of the turbine wheel, and Table 2 lists the salient non-dimensional turbine wheel parameters. The velocity triangles of the mean streamline of the turbine wheel are shown in Fig. 5.

Table 1 Turbine non-dimensional design parameters [2]

Parameter	Value
Specific speed, Ns	0.8 radians
Flow function, $W\sqrt{T_{\text{in}}}/P$	63.09 kg$\sqrt{}$K/s MPa
Specific work output ($C_p \Delta T/T_{\text{in}}$)	216.8 J/kg-K
Total-to-static pressure ratio	3.28
Total-to-static efficiency	73%

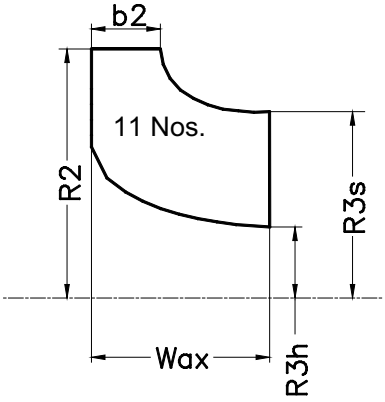

Fig. 4 Turbine wheel flow path [2]

Table 2 Turbine wheel design parameters [2]

Parameter	Value
R3h/R3s	0.38
R3s/R2	0.75
*b*2/*R*2	0.276
*U*2/*C*0	0.70
*V*3/*V*2	1.9
*C*3/*U*2	0.5

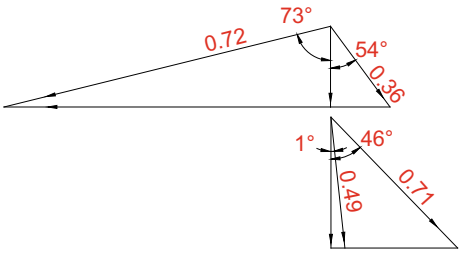

Fig. 5 Mean velocity triangle

3 Modelling and Grid Generation

The computational grid is generated using ICEM-CFD software [9]. The grids are unstructured tetrahedrals. Care is taken to ensure that sudden changes in geometry and flow are captured by locally introducing finer grids. After grid sensitivity analysis, the size of the volute grid is fixed at 2 million. The 3D computational grid used in the analysis for the volute is shown in Fig. 6.

The rotor domain is modelled such that it includes both the hub clearance and tip clearance regions. Whereas the tip clearance is contiguous from the inlet of the rotor to the exit, the hub clearance is partial. This calls for the hub region from the inlet to the end of scalloping to be modelled as a stationary wall with a clearance from the rotor blade and the heat shield wall. The region from the end of scalloping to the outlet is modelled as a rotating wall along with the rotor blades themselves. Due to such complexity, it is not possible for the grid generation process to be carried out in a template-based software such as ANSYS turbogrid.

Therefore, the modelling of the fluid domain a single rotor blade domain with partial hub clearance and full tip clearance is carried out in UG NX 10.0 software as shown in Fig. 7. The modelled geometry is exported to ICEM-CFD software, and grid is generated. The grids are blade-centered multi-block, structural hexahedrals. The grid topology is a combination of *O*, *C* and *H* topologies. The grids are made finer at the regions where high gradients are expected in the flow field.

The grid size for each rotor is fixed after the grid sensitivity analysis at 0.5 million. Figure 8 shows the grid independence plot for the rotor plotted against mass flow rate. Sufficient grid points are placed close to the aerofoil surfaces to resolve the boundary layer. The *y*+ values for the finalized grid are less than 12. The achieved skew angles

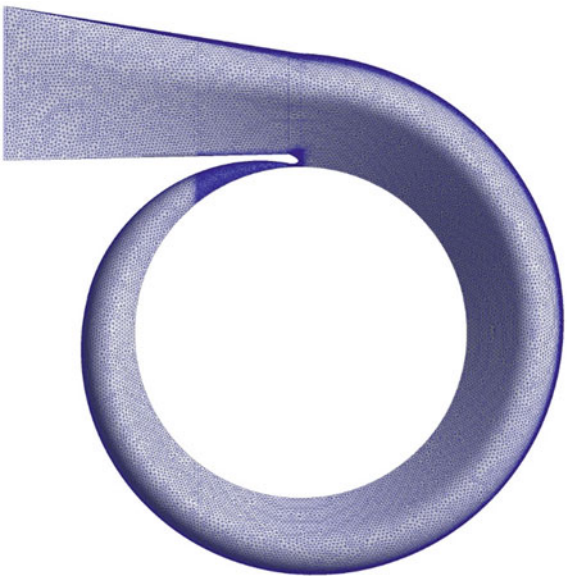

Fig. 6 3D computational grid of volute

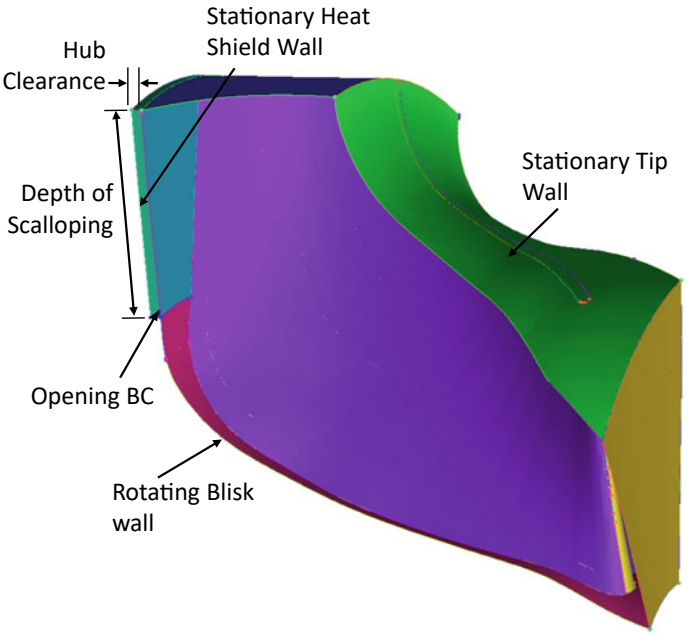

Fig. 7 Rotor blade domain

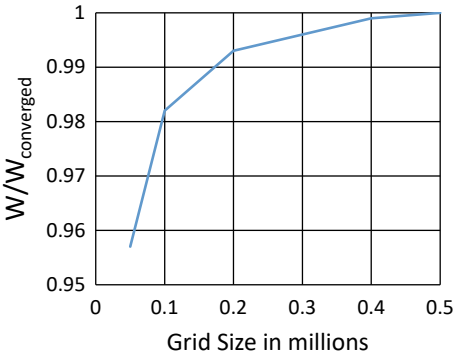

Fig. 8 Rotor grid independence plot

for the grids are between 30 and 150 degrees, the aspect ratios are less than 100, and expansion ratios are less than 1.2. The outlet domain of the grid is placed one chord downstream of the exit plane for the rotor grid. Multiple rotor meshes are generated to study five different depths of scalloping and three different hub clearances.

4 Computational Methodology

The analysis is carried out for the radial turbine by using the commercial 3D NS solver ANSYS CFX-19 [10] on an IBM DX 360 parallel computing system. The three-dimensional, multi-block, parallel flow solver CFX-19 developed by ANSYS is used for this analysis.

The Reynolds averaged Navier–Stokes equations are solved in the solution procedure. The governing equations are discretized using finite volume method. The solution algorithm is based on an implicit scheme coupled with multi-grid acceleration techniques. The effects of turbulence are modelled with two equations k-ω turbulence model with shear stress transport model. The significant advantage of this model is to predict improved wall shear stress in adverse pressure gradient flows and robustness for complex flows.

The boundary conditions are inlet total pressure, inlet total temperature, inlet flow angle and exit static pressure. The walls are assumed adiabatic. The blisk walls including the surface of the blade and the hub region from the end of scalloping to the outlet are treated as rotating walls. The tip clearance wall formed by the volute exit and the partial hub clearance wall created by the heat shield are treated as stationary walls. The clearance wall which bridges the hub clearance wall with the blisk wall separates the blade domain from the other side of the heat shield which is a closed chamber. Therefore, this is modelled as an opening across which the net mass flow is zero as shown in Fig. 7.

In order to capture the non-uniformity of the exit flow from the volute (especially at the tongue region), all the blades are modelled. Frozen rotor analysis is carried out

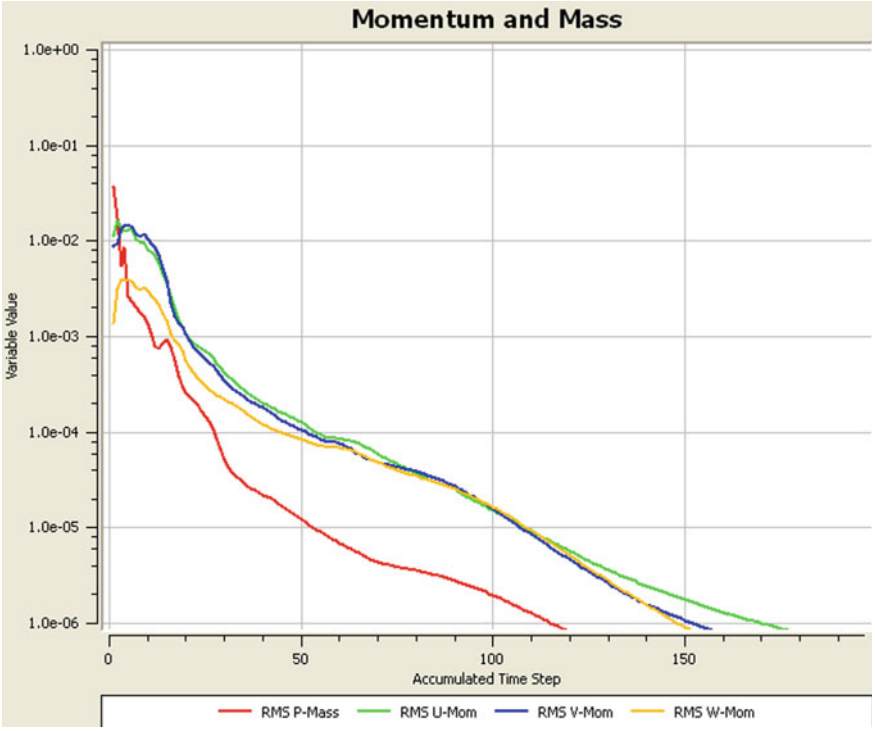

Fig. 9 Typical convergence history

for this purpose. The convergence criterion is set for the maximum residuals below 1E-4. The typical convergence history for the analysis is shown in Fig. 9.

5 Results and Discussion

3D NS analyses are carried out for various depths of scalloping and hub clearances with the finalized volute. The effect of the scalloping and hub clearance on the aerodynamic performance of the radial turbine stage is studied through the non-dimensional performance parameters of the turbine like mass flow function and efficiency.

All analyses are converged to same pressure ratio at the same non-dimensional turbine rotor speed function to enable comparison of the overall turbine stage parameters. The variation of efficiency with depth of scalloping is shown in Fig. 10.

Change in efficiency with increase in scalloping has been plotted against scalloping depth non-dimensionalized with hub meridional length. It can be observed that the drop in efficiency follows a nearly linear trend with increase in scalloping

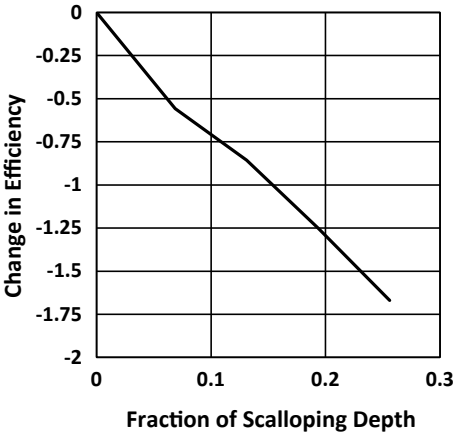

Fig. 10 Variation of efficiency with scalloping depth

depth. It is also seen that for an increase in depth of 25%, the efficiency reduces by about 1.75 percentage points.

As the depth of scalloping increases, the proportion of flow which cross-flows through the hub clearance region thereby not fully participating in the work production proportionally increases. This wasted flow can be visualized in the form of streamlines that are observed in the hub clearance region representing the cross-flow in Fig. 11. In a non-scalloped turbine wheel, this flow would be completely absent and the entire flow (minus the tip clearance flow) would pass through the turbine channel and contribute to work.

To observe the effect that such scalloping has in turbine work extraction, it is required to analyse the blade loading of the rotor blade near the hub. Figure 12

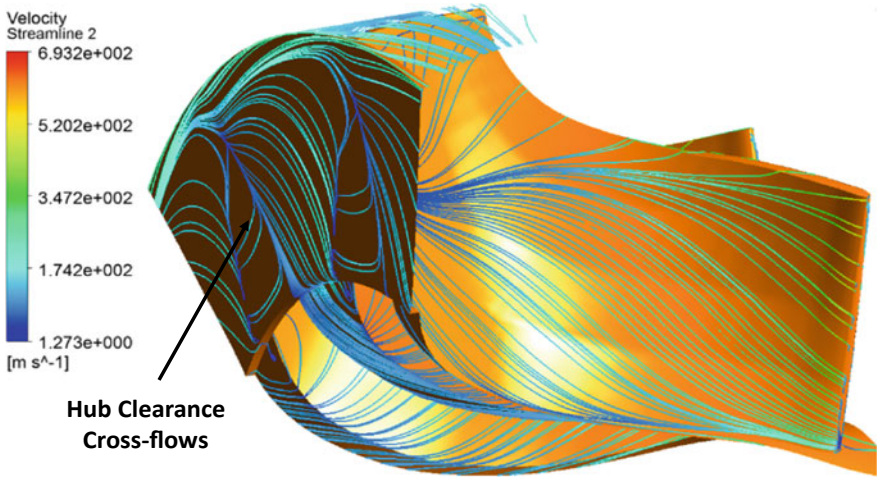

Fig. 11 Cross-flows in hub clearance region

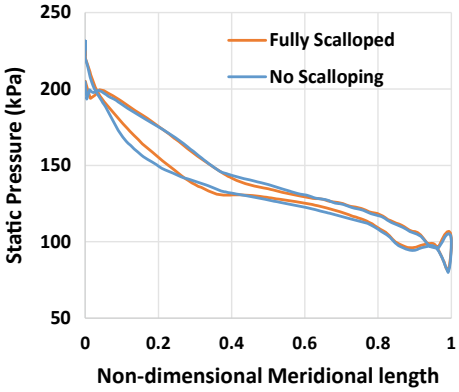

Fig. 12 Rotor blade loading

shows a comparison of blade loading of turbine blade at the hub location between a fully scalloped blade and a blade with no scalloping. The area enclosed by the blade loading curve is a measure of the work extracted by the turbine blade at this section.

As stated earlier, all analyses are converged for the same pressure ratio. It can be observed that the area enclosed by the curve is distinctly lesser in the case of the fully scalloped turbine blade as compared to the blade with no scalloping. Especially near the leading edge where the scalloping is done, this difference is marked. This translates to a reduction in power generated by the turbine which, for the same pressure ratio, translates to a reduction in stage efficiency as shown in Fig. 10.

To understand the effect of hub clearance on the performance of the radial turbine, analyses were carried out by varying the hub clearance values for a fixed depth of scalloping. Figure 13 shows the plot of hub clearance non-dimensionalized with inlet blade height versus change in efficiency. As expected, the efficiency decreases monotonically with increased hub clearance. It can be observed that the decrease in efficiency can be as high as 2.25% points in case of 8% hub clearance.

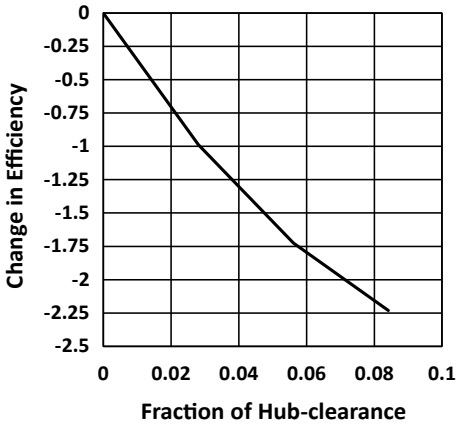

Fig. 13 Variation of efficiency with hub clearance

In the experimental investigation of the effect of various geometrical features of a radial turbine wheel on its performance, [8] observed that scalloping can contribute to a decrease in efficiency of 2 to 4 percentage points. This is in qualitative agreement with the numerical analyses that have been carried out as explained in this paper.

6 Conclusions

The effect of scalloping and hub clearance on the aerodynamic performance of a typical radial turbine stage of a turbocharger is studied using 3D NS analysis. Various depths of scalloping and hub clearances are modelled and meshed and analyzed using commercial software. It is observed that efficiency monotonically decreases with increase in both depth of scalloping and hub clearance. If the turbine wheel is scalloped to 25% of its meridional length, a drop in efficiency of 1.75 percentage points is observed. If the hub clearance is increased to 8% of inlet blade height, a drop in efficiency of 2.25% is observed. Thus, both of these parameters have considerable effect on the performance of the radial turbine and by extension, the turbocharger. The findings of this paper will help the designer to arrive at an optimal design which can take into account conflicting requirements such as aerodynamic efficiency, weight and inertia.

Acknowledgements The authors thank Director, GTRE, for giving permission to present this work.

References

1. Baines NC (2005) Fundamentals of turbocharging. Society of Automotive Engineers Inc
2. Bharathan RD, David John R, Sharad Kapil SV, Murty R, Kishore Prasad D (2017) Design and analysis of radial turbine for turbocharger application. In: Proceedings of the ASME Gas Turbine India Conference 2017
3. Rodgers C (1987) Small high pressure ratio radial turbine technology. VKI presentation
4. Rohlik H (1968) Analytical determination of radial inflow turbine design geometry for maximum efficiency. In: NASA-TN-D 4384
5. Whitfield A, Mohd Noor AB (1994) Design and performance of vaneless volutes for radial inflow turbines. Part 1: non-dimensional conceptual design considerations. Proc Instn Mech Engrs 208:199–211
6. Gu F, Engada A, Benisek A (2001) A comparative study of incompressible and compressible design approaches of radial inflow turbine volutes. Proc Instn Mech Engrs 215(A):475–486
7. Aungier RH (2006) Turbine aerodynamics: axial-flow and radial-inflow turbine design and analysis. ASME Press
8. Hiett GF, Johnston IH (1963) Experiments concerning the aerodynamic performance of inward flow radial turbines. Proc Instn Mech Engrs 1963–64:178
9. ICEM CFD 19.2; “User Documentation,”, ANSYS India Inc
10. ANSYS CFX 19.0; “User Documentation”, ANSYS India Inc